Commun. Theor. Phys. **72** (2020) 035405 (9pp) https://doi.org/10.1088/1572-9494/ab6912

Strong cosmic censorship for a scalar field in a logarithmic-de Sitter black hole

Yiqian Chen, Qingyu Gan[1] and Guangzhou Guo

Center for Theoretical Physics, College of Physics, Sichuan University, Chengdu, 610064, China

E-mail: chenyiqian@stu.scu.edu.cn, gqy@stu.scu.edu.cn and guangzhouguo@stu.scu.edu.cn

Received 18 November 2019, revised 3 January 2020
Accepted for publication 7 January 2020
Published 3 March 2020

Abstract

It has been shown that the quasinormal modes of perturebated fields can be used to investigate the validity of strong cosmic censorship (SCC). Relevant issues for Reissner–Nordstrom–de Sitter (RN-dS) black holes and Born–Infeld–de Sitter black holes have been discussed. In this paper, we investigate SCC in an asymptotic RN-dS black hole with logarithmic nonlinear electromagnetic field perturbed by massless scalar fields. It has been argued that SCC can be violated in a near-extremal RN-dS black hole. However, we find that the NLED effect can rescue SCC for a near-extremal logarithmic-de Sitter black hole. Compared with Born-Infeld model, we find that the NLED effect has similar behavior.

Keywords: logarithmic electrodynamics, quasinormal mode, strong cosmic censorship

(Some figures may appear in colour only in the online journal)

1. Introduction

The strong cosmic censorship (SCC) was proposed by Penrose to maintain the predictability of general relativity. As we know, a spacetime singularity can be formed by the gravitational collapse. Singularities can be classified as space-like singularities, light-like singularities and time-like singularities. For a spacetime with a time-like singularity, general relativity will lose its predictability because some regions in the space time can be influenced by the uncertain data on the singularity. To solve this problem, SCC asserts that, starting with some physically relevant initial data for Einstein's equation, the dynamics of physical systems will always produce globally hyperbolic spacetime [1–3]. In other words, a black hole formed by gravitational collapse or other physically acceptable dynamical procedure can only have space-like or light-like singularities, while time-like singularities are forbidden. However, some solutions of Einstein's equation possess time-like singularity, such as Reissner–Nordstrom black holes and Kerr–Newman black holes, which have Cauchy horizons. To fit with SCC, it is required that the perturbation for any fields at the Cauchy horizon is inextendible when physical initial data is perturbed. Therefore there is another statement of SCC: generally speaking, the maximal Cauchy development is inextendible.

However, the extendibility of the Cauchy horizon has some subtleties. For this reason, people proposed several formulated versions of SCC. If the perturbation (about the metric) arising from smooth initial data is C^{r} nondifferentiable at the Cauchy horizon, it is called C^{r} formulation of SCC [4, 5]. For example, the C^0 formulation demands that the perturbed metric to be noncontinuous at the Cauchy horizon. It indeed satisfies the requirement that the maximal Cauchy development is inextendible, yet has been proved to be wrong. There are also lots of discussions about the C^2 formulation which corresponds to the divergence of the curvature. Since the equations of motion are of the second order, it is reasonable that the curvature is required to be divergent at the Cauchy horizon. However, the C^2 formulation is still not appropriate. A macroscopic observer is able to cross the Cauchy horizon safely without being destroyed by a divergent curvature, therefore the C^2 formulation needs to be strengthened. With weak solutions showing many important physical applications, it becomes more reasonable to consider the weak solutions of the equations of motion. This idea leads to the Christodoulou's formulation of SCC [6], which will be adopted in the following discussion.

For simplicity, we put a test particle (field) into the spacetime without considering the back-reaction. For a linear massless scalar field, if SCC is implied, the scalar field perturbation will not belong to the Sobolev space H^1_{loc} at the

[1] Author to whom any correspondence should be addressed.

Cauchy horizon. Such fields have infinite energy at the Cauchy horizon. It has been proven that the Christodoulou's formulation is appropriate in the case of RN black holes and Kerr black holes. Generally speaking, when the scalar field propagates to the Cauchy horizon, it will experience an power-law decay [7–9], at the same time, there is an exponential blue-shift effect [10–15]. Ultimately, the dominant blue-shift effect would make the Cauchy horizon become singular [11, 16], therefore, SCC is respected for RN black holes and Kerr black holes. The above conclusion is based on the case that the cosmological constant Λ equals to 0. If we consider the spacetime with positive cosmological constant, situations will become quite different. The decay of the scalar field will be exponential rather than power-law near the Cauchy horizon [17–24]. So the validity of SCC depends on the competition between the exponential decay and blue-shift effect, which can be characterized by [25–30]

$$\beta = \frac{\alpha}{\kappa_-}, \tag{1.1}$$

where κ_- is the surface gravity of Cauchy horizon, and α is defined as $\inf_{\ln}\{-\mathrm{Im}\,(\omega_{\ln})\}$, where the $\omega_{\ln}$ is the quasinormal frequencies of the quasinormal modes (QNMs). (We will give more discussion at section 3.) The criterion is whether $\beta > \frac{1}{2}$ or not; if it is true, then Christodoulou's formulation of SCC is violated. It has been shown that SCC is respected in a Kerr–de Sitter (dS) black hole but violated in a near-extremal RN-dS black hole by a scalar field [30–33]. Violation of SCC in RN-dS black hole for various other fields, such as charged scalar field and Dirac field, are also discussed [34–38]. In [33], the author has shown a violation of SCC when a Kerr–dS black hole gets perturbed by Dirac fields. Besides, the validity of SCC is widely discussed in many other modified theories and black holes, such as Horndeski theory [39], the Martínez–Troncoso–Zanelli black hole [40] and higher-dimensional RN-dS black hole [41]. When considering the coupled linearized electromagnetic and gravitational perturbation, the violation of SCC will be severer in a RN-dS black hole [42]. What's more, it has been shown that nonlinear perturbations are not able to prevent SCC from being violated [43]. In addition, there is yet another way to save SCC in RN-dS black hole by the introduction of rough initial data which is shown in [44].

As we know, the RN metric is a solution of Einstein–Maxwell gravity, which has the infinite self-energy for charged point-like particles. Moreover, a point charge can not only lead to the electromagnetic singularity, but also the spacetime singularity through the gravitational field equations. Before renormalization, a classical approach has been proposed to solve this problem, namely the nonlinear electrodynamics (NLED). This approach was later generalized and applied to many other problems, like the limiting curvature hypothesis in cosmological theories and the vacuum polarization effect [45–47]. NLED was first introduced in the 1930s by Born and Infeld (BI). In addition to the above advantages, their NLED can also serve as a low energy effective limit of the superstring theory and play roles in the AdS/CFT correspondence [48]. Various NLED modes have been proposed and investigated for different purposes, such as exponential electrodynamics and logarithmic electrodynamics [49–52]. In this paper, we investigate the logarithmic electrodynamics, which can also remove the infinite self-energy. Although it does not have a background in superstring theory, it is still a good toy model to study various interesting subjects. When expanded to the second order of the NLED parameter, the action of logarithmic electrodynamics is consistent with that of the BI electrodynamics [53].

Two of us have discussed the validity of SCC in a BI-dS black hole in [54]. In order to explore the similarities and differences among different NLED effects, we further investigate SCC in a logarithmic-dS black hole. Our numerical results show that NLED effect of the BI electrodynamics and the logarithmic electrodynamics are similar in essential while differ in minor points. The most important conclusion is that the NLED effect can restore SCC in the near-extremal regime, which is violated in the RN-dS black hole.

In section 2, we review the logarithmic black hole solution. In section 3, we introduce the QNMs method. In section 4, we present our numerical results and give some discussions. It is worth mentioning that our analysis is based on the Christodoulou's formulation of SCC, and we set $16\pi G = c = 1$ throughout this paper.

2. Logarithmic-dS black hole

In this section, we review the black hole solution with logarithmic electromagnetic field. Then we find the parameter regions which allow three horizons so that the Cauchy horizon exists.

First let us begin with the action with logarithmiac electromagnetic field

$$S = \int \mathrm{d}^4x\sqrt{-g}\,[\mathcal{R} - 2\Lambda + L(\mathcal{F})], \tag{2.2}$$

$$L(\mathcal{F}) = -8b^2\ln\left(1 + \frac{\mathcal{F}}{8b^2}\right), \tag{2.3}$$

where $\mathcal{R}$ is the Ricci scalar, $\mathcal{F} = F_{\mu\nu}F^{\mu\nu}$, $F_{\mu\nu} = \partial_\mu A_\nu - \partial_\nu A_\mu$ is the electromagnetic field, A_μ is the corresponding electromagnetic potential, and b is the NLED parameter. NLED effect will magnify as the parameter b becomes small. On the contrary, NLED effect will reduce when the parameter b increases. The logarithmic electrodynamics recovers Maxwell electrodynamics in the limit of $b \to \infty$.

Varying the action (2.2), it is not hard to get the equations of motion

$$R_{\mu\nu} - \frac{1}{2}g_{\mu\nu}(R - 2\Lambda) = \frac{1}{2}g_{\mu\nu}L(\mathcal{F}) - 2F_{\mu\sigma}F_\nu{}^\sigma L_\mathcal{F}, \tag{2.4}$$

$$\partial_\mu(\sqrt{-g}\,L_\mathcal{F}F^{\mu\nu}) = 0, \tag{2.5}$$

where $R_{\mu\nu}$ is the Ricci tensor, and $L_\mathcal{F} \equiv \frac{\mathrm{d}L(\mathcal{F})}{\mathrm{d}\mathcal{F}}$. To demand a static spherically symmetric black hole solution, the metric of the logarithmic-dS black hole was obtained in [55]

$$\mathrm{d}s^2 = -f(r)\mathrm{d}t^2 + \frac{\mathrm{d}r^2}{f(r)} + r^2(\mathrm{d}\theta^2 + \sin^2\theta\mathrm{d}\varphi^2),$$

$$f(r) = 1 - \frac{(\Lambda - 4b^2)r^2}{3} - \frac{M}{8\pi r} + \frac{8b^2}{9}r^2\left(1 - {}_2F_1\left[-\frac{1}{2}, -\frac{3}{4}; \frac{1}{4}; -\frac{Q^2}{b^2r^4}\right]\right) - \frac{4b^2}{3}r^2\left(\sqrt{\frac{Q^2}{b^2r^4} + 1} - \log\left(\frac{Q^2}{2b^2r^4}\right) + \log\left(\sqrt{\frac{Q^2}{b^2r^4} + 1} - 1\right)\right). \tag{2.6}$$

After fixing gauge, the logarithmic electromagnetic potential is

$$\mathbf{A} = A_t \mathrm{d}t = \frac{2Q}{3r}\left(\frac{1}{1 + \sqrt{1 + \frac{Q^2}{r^4b^2}}} - 2{}_2F_1\left[\frac{1}{4}, \frac{1}{2}; \frac{5}{4}; -\frac{Q^2}{b^2r^4}\right]\right)\mathrm{d}t, \tag{2.7}$$

here ${}_2F_1$ is the hypergeometric function, M and Q are the mass and electric charge of the logarithmic-dS black hole, respectively. In the limit of $b \to \infty$, the metric (2.6) and the electromagnetic potential (2.7) recover the RN-dS black hole solution as expected.

To investigate SCC, we need to calculate QNMs at the Cauchy horizon, hence we only focus on the logarithmic-dS black holes which possess three horizons. It means that we need to find out the allowed parameter region where $f(r) = 0$ has three positive solutions, which correspond to the positions of the Cauchy horizon r_-, the event horizon r_+ and the cosmological horizon r_c, respectively. Because of the complexity of $f(r)$, we can only find the allowed region by numerical method and a bit analysis. First of all, through numerical simulation, we find that an appropriate $f(r)$ always has two extreme points $r_{\min}$ and $r_{\max}$, which does not coincide with zero points, namely, $f(r_{\min}) < 0$ and $f(r_{\max}) > 0$. It is noteworthy that there are extremal black hole solutions with $r_- = r_+$ and $f(r_{\min}) = 0$, in which situation we denote the charge of black hole as Q_{ext}. Similarly, there are solutions with $r_+ = r_c$ and $f(r_{\max}) = 0$, known as the Nariai black holes [56, 57]. These solutions form the bounds of the allowed region in the parameter space. Note that $f(r) \to -\infty$ in the limit $r \to +\infty$, therefore, $f(r)$ is supposed to be positive in the limit $r \to 0$. We expand $f(r)$ near $r = 0$ as follows

$$f(r) = \left(-\frac{M}{8\pi} + \frac{4bQ\Gamma\left(\frac{1}{4}\right)^2\sqrt{\frac{Q}{b}}}{9\sqrt{\pi}}\right)r^{-1} + \left(-\frac{4bQ}{3} + \frac{2bQ\Gamma\left(-\frac{1}{4}\right)}{3\Gamma\left(\frac{3}{4}\right)} + 1\right) + O(r), \tag{2.8}$$

where Γ is the Gamma function. Hence we get a relation

$$-\frac{M}{8\pi} + \frac{4bQ\Gamma^2\left(\frac{1}{4}\right)\sqrt{\frac{Q}{b}}}{9\sqrt{\pi}} > 0. \tag{2.9}$$

For simplicity, we take $M = 16\pi$ from now on without losing generality. The constraint (2.9) between Q and b becomes

$$bQ^3 > k, \quad k = \frac{81\pi}{4\Gamma^2\left(\frac{1}{4}\right)}. \tag{2.10}$$

Based on the above analysis, we plot the allowed region with three horizons in figure 1. As shown in the figure, the case $\Lambda = 0.02$ is different from the case $\Lambda = 0.14$. The parameter space of $\Lambda = 0.14$ has Nariai black holes, while the parameter space of $\Lambda = 0.02$ does not. Actually, this is not unique to the logarithmic-dS black holes. RN-dS black holes also have the similar conclusion. However, we will only be interested in the region near P, then the difference between various Λ is not significant. Near the point P, the allowed region is bounded by the upper bound (the green dashed line) and lower bound (the red dashed line).

3. Quasinormal mode

To investigate SCC, we need to take a test field as a probe to perturb the logarithmic-dS black hole. In this section, let us consider a scalar field perturbation with mass μ and charge q. The equation of motion of the field is the Klein–Gordon equation in a curved spacetime

$$(\mathbf{D}^2 - \mu^2)\Phi = 0, \tag{3.11}$$

where $\mathbf{D}$ is the covariant derivative $\mathbf{D} = \boldsymbol{\nabla} - \mathrm{i}q\mathbf{A}$. We make a transformation $v \equiv t + r_*$, where r_* is the tortoise coordinate defined as

$$r_* = \int \frac{\mathrm{d}r}{f(r)}. \tag{3.12}$$

Then we define the Eddington–Finkelstein ingoing coordinates (v, r, θ, φ) like in [42], so that we can discuss the properties of horizons more straightforward. Moreover, the gauge fixed logarithmic electromagnetic potential is

$$\mathbf{A} = A_v \mathrm{d}v = \frac{2Q}{3r}\left(\frac{1}{1 + \sqrt{1 + \frac{Q^2}{r^4b^2}}} - 2{}_2F_1\left[\frac{1}{4}, \frac{1}{2}; \frac{5}{4}; -\frac{Q^2}{b^2r^4}\right]\right)\mathrm{d}v. \tag{3.13}$$

Since we demand the logarithmic-dS black hole solution to be static and spherically symmetric, we can separate the field solution as the standard ansatz

$$\Phi = \mathrm{e}^{-\mathrm{i}\omega v}Y_{lm}(\theta, \phi)\psi_{\omega l}(r), \tag{3.14}$$

where $Y_{lm}(\theta, \phi)$ is the spherical harmonic function, and $\psi_{\omega l}(r)$ is the radial function. Plugging the ansatz (3.14) into the equation of motion (3.11), we get the radial equation

$$0 = [r^2 f\partial_r^2 + (r^2 f' + 2rf - 2\mathrm{i}qA_v r^2 - 2\mathrm{i}\omega r^2)\partial_r - 2\mathrm{i}\omega r - 2\mathrm{i}qrA_v - \mathrm{i}qr^2\partial_r A_v - l(l+1) - \mu^2 r^2]\psi_{\omega l}(r), \tag{3.15}$$

where f' denotes $\mathrm{d}f(r)/\mathrm{d}r$. For the convenience of numerical calculation, we define a new coordinate

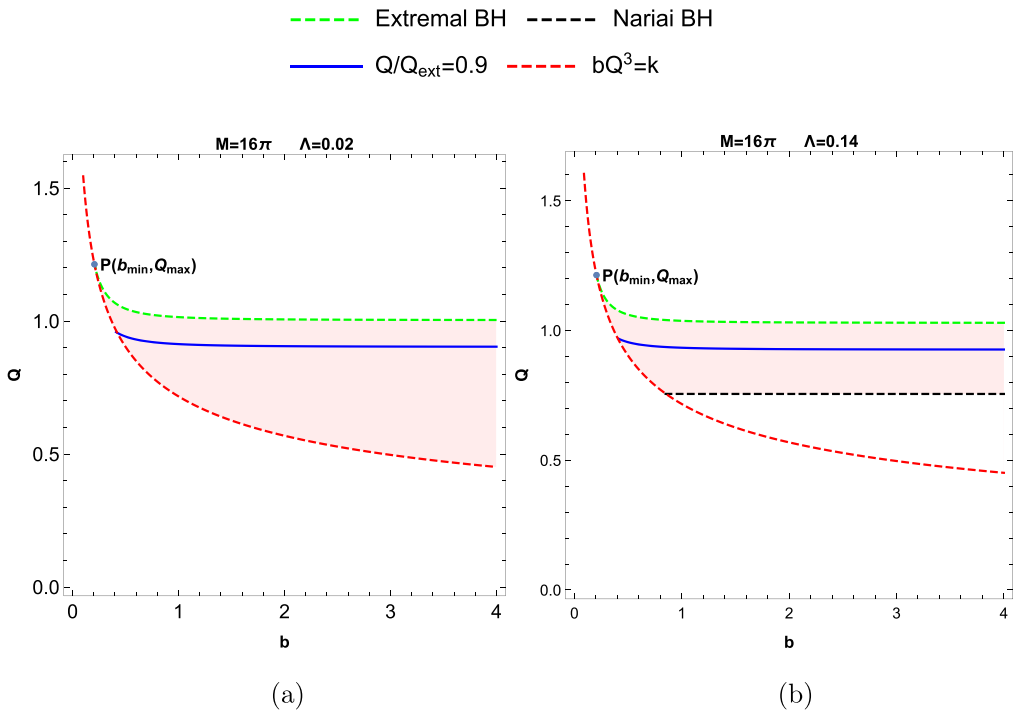

Figure 1. Parameter space for logarithmic-ds black holes with $M = 16\pi$. (a) $\Lambda = 0.02$. (b) $\Lambda = 0.14$. The pink region allows for black holes with three horizons. The dashed green lines represent the extremal black holes with $r_- = r_+$; the dashed black line represents the Nariai black hole with $r_+ = r_c$; and the dashed red lines represent the constraint $bQ^3 = k$. We can see the dashed red line and the dashed green line intersect at the point $P(b_{\min}, Q_{\max})$. Here, $b_{\min} \approx 0.206\,008$ and $Q_{\max} \approx 1.213\,543$ are calculated by numerical method which does not depend on Λ (an analytic expression will be given in the section 4). The blue line represent near-extremal black holes with charge $Q = 0.9Q_{\text{ext}}$, where Q_{ext} is the charge of a extremal black hole with the same b.

Table 1. The lowest-lying QNMs ω/κ_- of different angular numbers l for various values of Λ, b, Q/Q_{ext} and q for massless scalar perturbation. In the large b limit ($b = 10\,000$), the numerical results go back to that of the RN-dS black holes [30, 34].

Λ	b	Q/Q_{ext}	q	$l = 0$	$l = 1$	$l = 10$
0.02	0.5	0.991	0	0	−0.472 594i	±14.968 405 − 0.467 179i
			0.1	0.059 183 + 0.003 005i	0.033 367 − 0.471 978i	15.286 357 − 0.467 124i
		0.996	0	0	±3.605 333 − 0.789 770i	±25.275 405 − 0.770 342i
			0.1	0.099 702 + 0.005 331i	4.165 818 − 0.779 759i	25.818 396 − 0.769 624i
	10000	0.991	0	0	−0.475 688i	±14.365 381 − 0.491 756i
			0.1	0.057 773 + 0.002 229i	0.032 203 − 0.475 118i	−14.080 016 − 0.491 441i
		0.996	0	0	−0.789 379i	±23.969 407 − 0.808 962i
			0.1	0.096 356 + 0.003 870i	0.053 708 − 0.788 423i	−23.488 922 − 0.808 825i
0.06	0.5	0.991	0	0	±2.021 008 − 0.458 730i	±14.396 115 − 0.441 376i
			0.1	0.128 077 + 0.003 969i	2.384 318 − 0.452 275i	14.744 827 − 0.441 085i
		0.996	0	0	±3.431 580 − 0.759 489i	±24.467 637 − 0.730 447i
			0.1	0.216 661 + 0.007 511i	4.054 003 − 0.743 932i	25.066 143 − 0.729 315i
	10 000	0.991	0	0	±1.930 716 − 0.481 345i	±13.798 347 − 0.462 716i
			0.1	0.127 461 + 0.001 895i	2.265 562 − 0.474 726i	14.119 498 − 0.462 581i
		0.996	0	0	±3.242 616 − 0.795 833i	±23.189 760 − 0.764 924i
			0.1	0.213 619 + 0.003 591i	3.808 829 − 0.781 460i	23.733 891 − 0.764 259i

$x \equiv (r - r_+)/(r_c - r_+)$, such that the event horizon and cosmological horizon are located at $x = 0$, 1, respectively. Through the Frobenius method, we can impose the boundary solutions near the event horizon and the cosmological horizon. Near the event horizon, the ingoing and outgoing boundary solutions are

$$\psi_{\omega l}^{\text{ingoing}} \sim \text{const}, \quad \psi_{\omega l}^{\text{outgoing}} \sim x^{\mathrm{i}\frac{\omega + qA_v|_{r=r_+}}{\kappa_+}}. \tag{3.16}$$

Similarly, near the cosmological horizon, the ingoing and outgoing boundary solutions are

$$\psi_{\omega l}^{\text{ingoing}} \sim \text{const}, \quad \psi_{\omega l}^{\text{outgoing}} \sim (1 - x)^{-\mathrm{i}\frac{\omega + qA_v|_{r=r_c}}{\kappa_c}}, \tag{3.17}$$

where $\kappa_h \equiv |f'(r_h)|/2$ denotes the surface gravity at each horizon with $h \in \{+,-,c\}$. We impose the ingoing boundary solution of (3.16) at the event horizon and the outgoing boundary solution of (3.17) at cosmological horizon. These

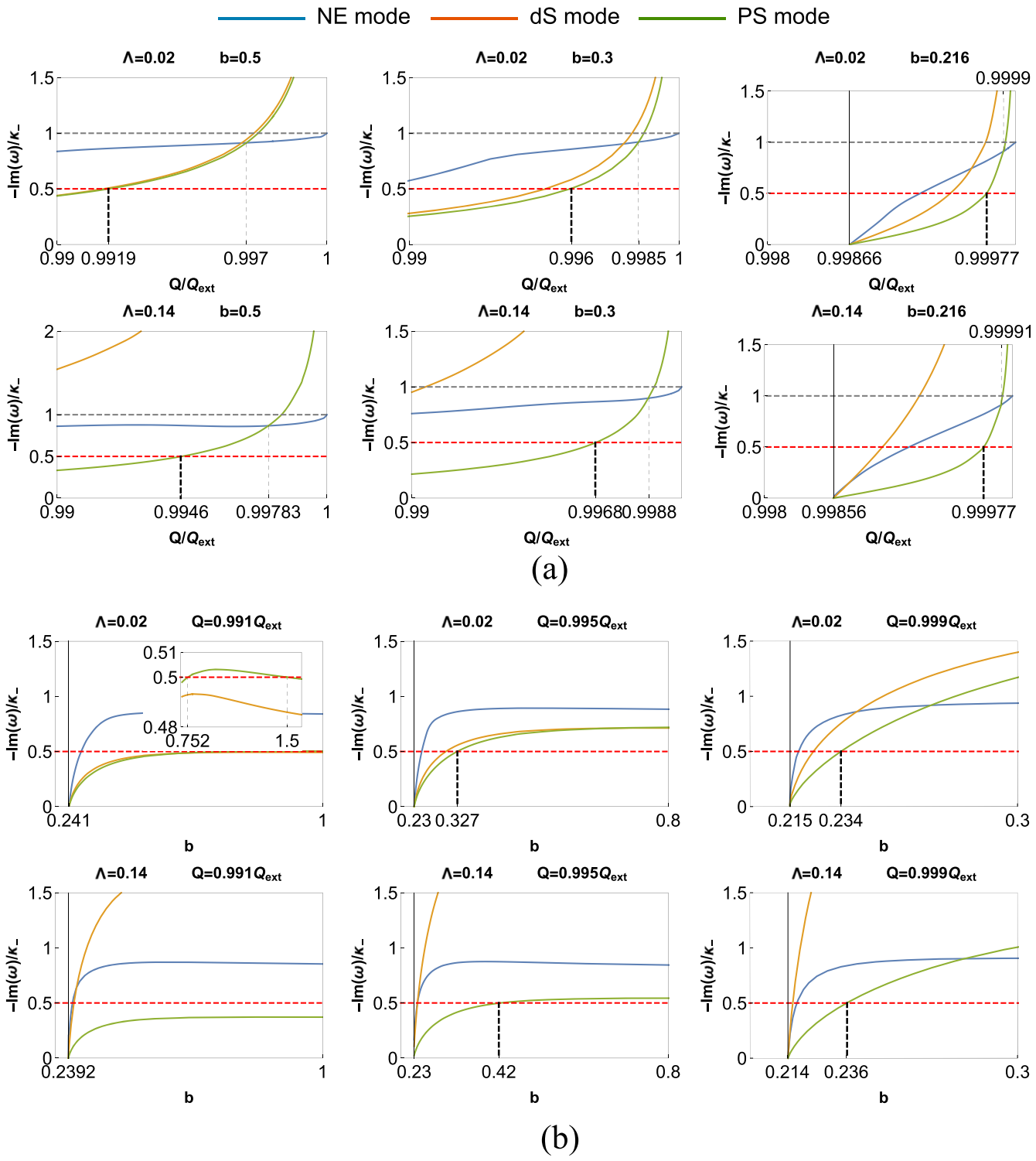

Figure 2. The lowest-lying QNMs $-\mathrm{Im}(\omega)/\kappa_-$ of three families for a neutral massless scalar field. The vertical solid lines indicate that the parameters reach the lower bound of allowed region, where the logarithmic-dS black hole does not have three horizons. SCC is violated only when the dominant modes of three families are all above the red dashed line. And the thick black dashed lines indicate the key points where $\beta \equiv -\mathrm{Im}(\omega)/\kappa_- = \frac{1}{2}$. (a) The lowest-lying QNMs $-\mathrm{Im}(\omega)/\kappa_-$ of three families with varying Q/Q_{ext} for various values of b and Λ. The vertical thin dashed lines indicate that the NE modes become dominant. On the right side of the thick dashed lines, we can see that SCC is violated. (b) The lowest-lying QNMs $-\mathrm{Im}(\omega)/\kappa_-$ of three families with varying b for various values of Q/Q_{ext} and Λ. Near the vertical solid thin lines, we can see that SCC is always respected for a small enough value of b.

conditions select a discrete set of frequencies ω_{ln}, namely the quasinormal frequencies, where l is the angular number, and n is the mode number. The corresponding modes are called QNMs. It is noteworthy that there is a zero mode when $l = 0$, which should be ignored [30]. In fact, there are a variety of methods to compute the QNMs. Our numerical results in section 4 are based

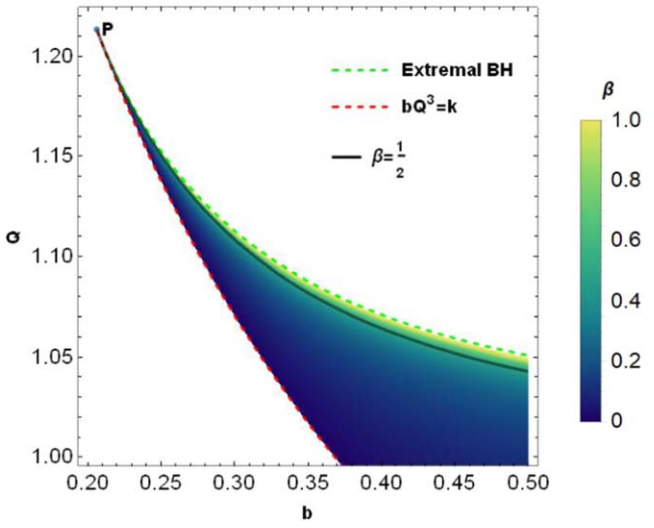

Figure 3. β for a neutral massless scalar field with $M = 16\pi$, and $\Lambda = 0.06$. The green dashed line and the red dashed line correspond to the extremal black hole ($Q = Q_{\rm ext}$) and lower bound ($bQ^3 = k$) of the allowed region, respectively. The solid thick black line represents $\beta = \frac{1}{2}$, which divides the parameter space into two parts, where SCC is violated above the black line while respected under it.

on the Chebyshev collocation scheme, and obtained mostly by the Mathematica package provided in [58–60]. In order to fit the numerical scheme, we redefine the field $\psi_{\omega l}$ as

$$\psi_{\omega l} = \frac{1}{x}(1-x)^{-\mathrm{i}\frac{\omega+qA_v|_{r=r_c}}{\kappa_c}}\phi_{\omega l}, \tag{3.18}$$

so that the redefined field $\phi_{\omega l}$ become regular at both the event horizon and the cosmological horizon.

To see the criterion $\beta > \frac{1}{2}$, we should get the boundary solutions of the equation of motion (3.15) at the Cauchy horizon. As shown in [32], scalar field perturbation will diverge as $v \to -\infty$, if we use ingoing coordinates. Therefore, we work out the two independent boundary solutions in the outgoing coordinates (u, r, θ, φ)

$$\psi^1_{\omega l} \sim \text{const}, \quad \psi^2_{\omega l} \sim (r-r_-)^{\mathrm{i}\frac{\omega+qA_u|_{r=r_-}}{\kappa_-}}.$$

Similar to analysis in [32], the square integrability of $\partial_r\psi_{\omega l}$ gives us the criterion $\beta > \frac{1}{2}$.

4. Numerical results

In this section, we present our numerical results. In the first subsection, we discuss the validity of SCC with massless neutral scalar perturbations; in the second subsection, we discuss the validity of SCC with massless charged scalar perturbations. Since the NLED effect is strong when b is relatively small, SCC is most likely to be violated in near-extremal black holes. We are hence more interested in the black holes which are near the point P in the parameter space.

To verify the reliability of the program, we calculated a series of lowest-lying QNMs in table 1. Comparing our results with that of RN-dS black holes [30, 34], we find that they are consistent for large b ($b = 10\,000$).

4.1. Neutral scalar field

Since it is impossible to calculate ω_{ln} for all l and n, a clever method was proposed to seek out the lowest-lying QNMs for RN-dS black holes [30]. The authors found three different families that can classify the QNMs: the photon sphere (PS) modes, with dominant mode at large l ($l = 10$ is good enough); the dS modes, with dominant mode at $l = 1$; and the near-extremal (NE) modes, with dominant mode at $l = 0$. The PS among them also has been discussed in [61]. In the process of numerical calculation, we also find these three distinct families of modes for a neutral massless scalar field in the logarithmic-dS black hole, therefore, we are going to discuss the neutral case by these three families in this subsection.

Before talking about SCC for near-extremal black hole, we first investigate the behavior near the lower bound given by constraint ((2.10) i.e. the red dashed line in figure 1). We find that the radius r_- goes to zero in the limit of $bQ^3 \to k$, so we can expand the surface gravity of Cauchy horizon around $r_- = 0$ as follows

$$\kappa_- = \left|\frac{1}{2r}\frac{\mathrm{d}(rf(r))}{\mathrm{d}r}|_{r=r_-}\right| = \frac{1-4Qb}{2r_-} + O(1). \tag{4.19}$$

Therefore as long as $1 - 4Qb \neq 0$, κ_- will go to infinity at the lower bound. Indeed, the condition $1 - 4Qb = 0$ and the condition $bQ^3 = k$ intersect at the point $P(b_{\rm min}, Q_{\rm max})$, where

$$b_{\rm min} = \frac{4\sqrt{\pi}\Gamma\left(\frac{1}{4}\right)^2}{9M}, \quad Q_{\rm max} = \frac{9M}{16\sqrt{\pi}\Gamma\left(\frac{1}{4}\right)^2}.$$

We find α are finite at the lower bound, hence $\beta = 0 < \frac{1}{2}$. It means that SCC is always respected for the black holes whose parameters are close enough to the lower bound (this conclusion is also reflected in figure 2 as explained below).

We plot the lowest-lying QNMs $-\mathrm{Im}(\omega)/\kappa_-$ of three families in figure 2, where the blue line represents the dominant mode of NE family ($l = 0$), the orange line represent the dominant mode of dS family ($l = 1$), the green line represents the dominant mod of PS family ($l = 10$). In figure 2(a), we plot $-\mathrm{Im}(\omega)/\kappa_-$ against $Q/Q_{\rm ext}$ and find that the lowest-lying QNMs of PS and dS families go to infinite while the modes of NE family go to 1. This behavior not only indicates that the NE modes become dominant for a sufficiently near-extremal black hole, but also implies that SCC can always be violated for a sufficiently near-extremal black hole. Moreover, we find that the critical $Q/Q_{\rm ext}$ of $\beta = \frac{1}{2}$ increase as b decrease, which means that SCC is more difficult to be violated as b decreases. In figure 2(b), we plot $-\mathrm{Im}(\omega)/\kappa_-$ against b for some fixed $Q/Q_{\rm ext}$. First of all, the most noticeable feature is that the lowest-lying QNMs of the three families approach 0 at $b = b_{Q/Q_{\rm ext}}$, which is consistent with the analysis in the last paragraph. Here, $b_{Q/Q_{\rm ext}}$ is the minimal b for a fixed charge ratio $Q/Q_{\rm ext}$, namely the intersection of the line of fixed $Q/Q_{\rm ext}$ and the lower bound as show in figure 1. In the case of $\Lambda = 0.14$, $Q = 0.991Q_{\rm ext}$, the

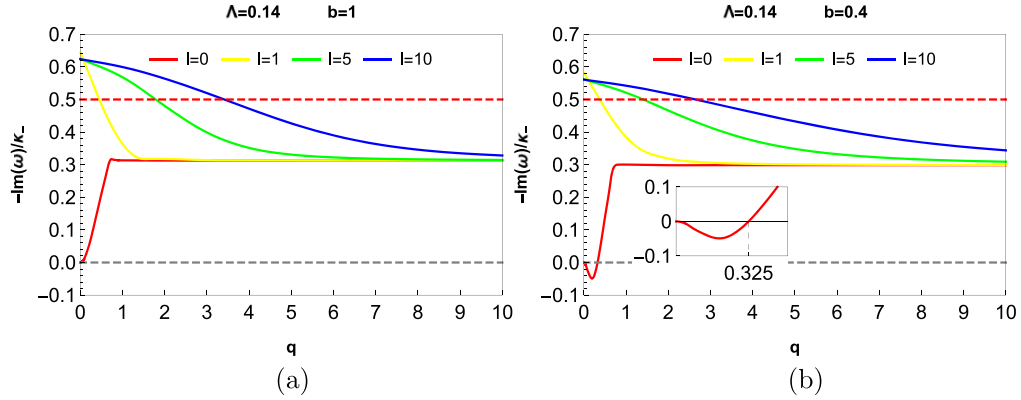

Figure 4. The lowest-lying QNMs $-\mathrm{Im}(\omega)/\kappa_-$ of various values of l with varying q for $\Lambda = 0.14$ and $Q = 0.996Q_{\mathrm{ext}}$. (a) $b = 1$. (b) $b = 0.4$, where the small figure zooms in the superradiance.

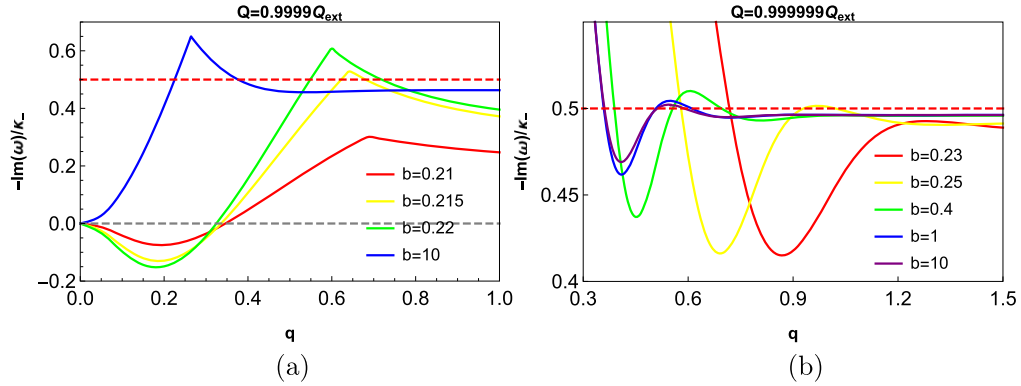

Figure 5. The lowest-lying QNMs $-\mathrm{Im}(\omega)/\kappa_-$ of $l = 0$ with varying q for $\Lambda = 0.14$ and various values of b. (a) $Q = 0.9999Q_{\mathrm{ext}}$. (b) $Q = 0.999\,999Q_{\mathrm{ext}}$.

lowest-lying PS mode is lower than the red dashed line for any b, therefore SCC is always respected. Similarly, in the case of $\Lambda = 0.02$, $Q = 0.991Q_{\mathrm{ext}}$, although the lowest-lying PS mode fluctuates around $\beta = \frac{1}{2}$, the dominant dS mode save the validity of SCC. In summary, $\boldsymbol{b}$ and Q/Q_{ext} both have important effects on the validity of SCC. Specifically, SCC is more likely to be violated when Q/Q_{ext} goes to 1, and more likely to be respected when b goes to $b_{Q/Q_{\mathrm{ext}}}$.

At the end of this subsection, in order to understand the behavior of β more intuitively, we roughly draw a density plot of β near the point P by WKB method in figure 3. In this figure, we use the PS modes to approximate β of nonextremal black holes, where dS modes are similar to PS modes and NE modes are not dominant. The solid black line, the red dashed line and the green dashed line represent $\beta = \frac{1}{2}$, 0, and 1, respectively. Note that, SCC is violated between the green line and the black line $\left(0 < \beta < \frac{1}{2}\right)$, while respected between the red line and the black line $\left(\frac{1}{2} < \beta < 1\right)$.

4.2. Charged scalar field

Now we investigate the validity of SCC for a massless charged scalar field. Unlike the neutral case, we do not use the three families to classify the QNMs. Since the violation of SCC is more likely to occur in a near-extremal black hole, we only consider some near-extremal black holes in the following. In figure 4, we plot the lowest-lying QNMs $-\mathrm{Im}(\omega)/\kappa_-$ of various angular number l in near-extremal logarithmic-dS black holes. It is easy to find that the lowest-lying QNMs of $l = 0$ (red line) dominate β for the charged scalar field in near-extremal black holes. In the case of $b = 0.4$, it is noteworthy that the lowest-lying QNMs can be negative when scalar charge q is small. Actually, this abnormality has been found in RN-dS black holes, and was regarded as superradiant instability [62, 63]. It is improper to infer anything about SCC when superradiance occurs, since the perturbations will be severely unstable even in the exterior of the black hole in this case. Note that, the $l = 0$ zero mode is trivial and should be ignored in the limit of $q \to 0$, so the subdominant mode of $l = 0$ should be considered like in [34]. For a nonzero q, we can confirm that SCC is respected, due to the nontrivial lowest-lying of $l = 0$.

Since the lowest-lying QNMs of $l = 0$ dominate β for the charged scalar field in a near-extremal black hole, we now focus on the $l = 0$ mode for black holes further near the extremality. In figure 5, we plot the lowest-lying QNMs of $l = 0$ with varying q for $\Lambda = 0.14$. The (a) panel of figure 5 shows the case of $Q = 0.9999Q_{\mathrm{ext}}$. The blue line represents the black hole of $b = 10$, which is almost identical to the case of RN-dS black hole. For $b = 10$, 0.22 and 0.215, we can find a narrow scalar charge window, where SCC is violated. Interestingly, as b decreases, the violation regime decreases, and for $b = 0.21$, the violation regime totally disappears.

What's more, in the (b) panel of figure 5, with $Q = 0.999\,999 Q_{\rm ext}$, we can find wiggles near $\beta = \frac{1}{2}$ in the cases of $b = 10$, 1, 0.4 and 0.25, while in the case of $b = 0.23$ the wiggle disappears. The presence of the wiggles has been discussed in detail in the RN-dS black holes in [35]. We also find that the wiggle shifts towards the direction of q increasing as b decreases.

5. Conclusion

In this paper, we investigate the validity of SCC for a massless scalar field in a logarithmic-dS black hole. We first make a brief discussion on the logarithmic-dS black holes and give the allowed region in which the Cauchy horizon exists in the section 2. After that we make some preparations for the calculation of QNMs in section 3. Finally, we present the numerical results of neutral scalar fields and charged scalar fields in section 4.

It is noteworthy that when b goes to infinity, the logarithmic-dS black hole will go back to the RN-dS black hole as expected. Therefore the behavior of SCC in a logarithmic-dS black hole is similar to that of a RN-dS black hole when b is big enough. When the NLED effect increases, however, we find some interesting behaviors of SCC which are different from RN-dS black hole. Through the analysis of the numerical results, we found that the NLED effect can to some extent rescue SCC for a near-extremal logarithmic-dS black hole. The specific impact of NLED effect on SCC is as follows.

For a massless neutral scalar field: firstly, as NLED effect increases, the minimal $Q/Q_{\rm ext}$ for which the violation of SCC emerges goes to 1; secondly, given a fixed $Q/Q_{\rm ext}$, the NLED effect can always rescue SCC as long as the parameter b goes to $b_{Q/Q_{\rm ext}}$.

For a massless charged scalar field: firstly, the NLED effect can lead to the appearance of superradiance; secondly, the NLED effect can eliminate the narrow scalar charge window where SCC is violated; thirdly, the NLED effect can eliminate the wiggles near $\beta = \frac{1}{2}$.

In general, no matter for the massless neutral scalar field or the massless charged scalar field, the NLED effect is able to rescue SCC. We find that the NLED effect of logarithmic-dS black holes can lead to the shifting of the wiggles which is not obsevered in the Born-Infeld case. Since the two NLED effects show great difference only when b tends to 0, it is reasonable that the two effects are similar with $b > b_{\rm min}$.

Acknowledgments

We are deeply grateful to Peng Wang and Bo Ning for their helpful discussions and suggestions. This work is supported in partial by NSFC (Grant No. 11505119, 11005016, 11875196 and 11375121).

References

[1] Penrose R 1969 Gravitational collapse: the role of general relativity *Riv. Nuovo Cim.* **1** 252–76
Penrose R 2002 Gravitational collapse: the role of general relativity *Gen. Relativ. Gravit.* **34** 1141
[2] Penrose R 1965 Gravitational collapse and space–time singularities *Phys. Rev. Lett.* **14** 57–9
[3] Hawking S W and Penrose R 1970 The Singularities of gravitational collapse and cosmology *Proc. R. Soc.* A **314** 529–48
[4] Luk J and Oh S-J 2017 Strong cosmic censorship in spherical symmetry for two-ended asymptotically flat initial data: I. The interior of the black hole region (arXiv:1702.05715)
[5] Luk J and Oh S-J 2017 Strong cosmic censorship in spherical symmetry for two-ended asymptotically flat initial data: II. The exterior of the black hole region (arXiv:1702.05716)
[6] Christodoulou D 2008 The formation of black holes in general relativity *On Recent Developments in Theoretical and Experimental General Relativity, Astrophysics and Relativistic Field Theories. Proc. 12th Marcel Grossmann Meeting on General Relativity* vol 1–3 *(Paris, France 12–18, July 2009)* pp 24–34
[7] Price R H 1972 Nonspherical perturbations of relativistic gravitational collapse: I. Scalar and gravitational perturbations *Phys. Rev.* D **5** 2419–38
[8] Dafermos M, Rodnianski I and Shlapentokh-Rothman Y 2014 Decay for solutions of the wave equation on Kerr exterior spacetimes: III. The full subextremal case |a| < M (arXiv:1402.7034)
[9] Angelopoulos Y, Aretakis S and Gajic D 2018 Late-time asymptotics for the wave equation on spherically symmetric, stationary spacetimes *Adv. Math.* **323** 529–621
[10] Chambers C M 1997 The Cauchy horizon in black hole de Sitter space-times *Ann. Isr. Phys. Soc.* **13** 33
[11] Dafermos M 2005 The Interior of charged black holes and the problem of uniqueness in general relativity *Commun. Pure Appl. Math.* **58** 0445–504
[12] Poisson E and Israel W 1990 Internal structure of black holes *Phys. Rev.* D **41** 1796–809
[13] Ori A 1991 Inner structure of a charged black hole: an exact mass-inflation solution *Phys. Rev. Lett.* **67** 789–92
[14] Hod S and Piran T 1998 Mass inflation in dynamical gravitational collapse of a charged scalar field *Phys. Rev. Lett.* **81** 1554–7
[15] Brady P R and Smith J D 1995 Black hole singularities: a numerical approach *Phys. Rev. Lett.* **75** 1256–9
[16] Dafermos M 2014 Black holes without spacelike singularities *Commun. Math. Phys.* **332** 729–57
[17] Bony J-F and Hafner D 2007 Decay and non-decay of the local energy for the wave equation in the de Sitter–Schwarzschild metric (arXiv:0706.0350)
[18] Dyatlov S 2015 Asymptotics of linear waves and resonances with applications to black holes *Commun. Math. Phys.* **335** 1445–85
[19] Dyatlov S 2012 Asymptotic distribution of quasi-normal modes for Kerr-de Sitter black holes *Ann. Henri Poincare* **13** 1101–66
[20] Hintz P and Vasy A 2016 The global non-linear stability of the Kerr–de Sitter family of black holes (arXiv:1606.04014)
[21] Hintz P 2016 Non-linear stability of the Kerr–Newman–de Sitter family of charged black holes (arXiv:1612.04489)
[22] Berti E, Cardoso V and Starinets A O 2009 Quasinormal modes of black holes and black branes *Class. Quantum Grav.* **26** 163001
[23] Konoplya R A and Zhidenko A 2011 Quasinormal modes of black holes: from astrophysics to string theory *Rev. Mod. Phys.* **83** 793–836

[24] Brady P R, Chambers C M, Krivan W and Laguna P 1997 Telling tails in the presence of a cosmological constant *Phys. Rev.* D **55** 7538–45
[25] Costa J L, Girão P M, Natário J and Silva J D 2017 On the global uniqueness for the Einstein–Maxwell-scalar field system with a cosmological constant: III. Mass inflation and extendibility of the solutions **2017** 8
[26] Costa J L, Girão P M, Natário J and Silva J D 2015 On the global uniqueness for the Einstein–Maxwell-scalar field system with a cosmological constant: I. Well posedness and breakdown criterion *Class. Quantum Grav.* **32** 015017
[27] Costa J L, Girão P M, Natário J and Silva J D 2015 On the global uniqueness for the Einstein–Maxwell-scalar field system with a cosmological constant *Commun. Math. Phys.* **339** 903–47
[28] Hintz P and Vasy A 2017 Analysis of linear waves near the Cauchy horizon of cosmological black holes *J. Math. Phys.* **58** 081509
[29] Kehle C and Shlapentokh-Rothman Y 2019 A scattering theory for linear waves on the interior of Reissner–Nordström black holes *Ann. Henri Poincare* **20** 1583–650
[30] Cardoso V, Costa J L, Destounis K, Hintz P and Jansen A 2018 Quasinormal modes and strong cosmic censorship *Phys. Rev. Lett.* **120** 031103
[31] Rahman M, Chakraborty S, SenGupta S and Sen A A 2019 Fate of strong cosmic censorship conjecture in presence of higher spacetime dimensions *J. High Energy Phys.* JHEP03(2019)178
[32] Dias O J C, Eperon F C, Reall H S and Santos J E 2018 Strong cosmic censorship in de Sitter space *Phys. Rev.* D **97** 104060
[33] Rahman M 2019 On the validity of strong cosmic censorship conjecture in presence of Dirac fields (arXiv:1905.06675)
[34] Mo Y, Tian Y, Wang B, Zhang H and Zhong Z 2018 Strong cosmic censorship for the massless charged scalar field in the Reissner–Nordstrom–de Sitter spacetime *Phys. Rev.* D **98** 124025
[35] Dias O J C, Reall H S and Santos J E 2019 Strong cosmic censorship for charged de Sitter black holes with a charged scalar field *Class. Quantum Grav.* **36** 045005
[36] Cardoso V, Costa J L, Destounis K, Hintz P and Jansen A 2018 Strong cosmic censorship in charged black-hole spacetimes: still subtle *Phys. Rev.* D **98** 104007
[37] Ge B, Jiang J, Wang B, Zhang H and Zhong Z 2019 Strong cosmic censorship for the massless Dirac field in the Reissner–Nordstrom–de Sitter spacetime *J. High Energy Phys.* JHEP01(2019)123
[38] Destounis K 2019 Charged fermions and strong cosmic censorship *Phys. Lett.* B **795** 211–9
[39] Destounis K, Fontana R D B, Mena F C and Papantonopoulos E 2019 Strong cosmic censorship in Horndeski theory *J. High Energy Phys.* JHEP10(2019)280
[40] Gwak B 2019 Strong cosmic censorship under quasinormal modes of non-minimally coupled massive scalar field *Eur. Phys. J.* C **79** 767
[41] Liu H, Tang Z, Destounis K, Wang B, Papantonopoulos E and Zhang H 2019 Strong cosmic censorship in higher-dimensional Reissner–Nordström–de Sitter spacetime *J. High Energy Phys.* JHEP03(2019)187
[42] Dias O J C, Reall H S and Santos J E 2018 Strong cosmic censorship: taking the rough with the smooth *J. High Energy Phys.* JHEP10(2018)001
[43] Luna R, Zilhao M, Cardoso V, Costa J L and Natario J 2019 Strong cosmic censorship: the nonlinear story *Phys. Rev.* D **99** 064014
[44] Dafermos M and Shlapentokh-Rothman Y 2018 Rough initial data and the strength of the blue-shift instability on cosmological black holes with $\Lambda > 0$ *Class. Quantum Grav.* **35** 195010
[45] Mukhanov V F and R H Brandenberger 1992 A Nonsingular universe *Phys. Rev. Lett.* **68** 1969–72
[46] Brandenberger R H, Mukhanov V F and Sornborger A 1993 A Cosmological theory without singularities *Phys. Rev.* D **48** 1629–42
[47] Heisenberg W and Euler H 1936 Consequences of Dirac's theory of positrons *Z. Phys.* **98** 714–32
[48] Fradkin E S and Tseytlin A A 1985 Nonlinear electrodynamics from quantized strings *Phys. Lett.* B **163** 123–30
[49] Wang P, Wu H and Yang H 2019 Holographic DC conductivity for backreacted nonlinear electrodynamics with momentum dissipation *Eur. Phys. J.* C **79** 6
[50] Wang P, Wu H and Yang H 2019 Thermodynamics and phase transitions of nonlinear electrodynamics black holes in an extended phase space *J. Cosmol. Astropart. Phys.* JCAP04(2019)052
[51] Wang P, Wu H and Yang H 2019 Thermodynamics and weak cosmic censorship conjecture in nonlinear electrodynamics black holes via charged particle absorption (arXiv:1904.12365)
[52] Wang P, Wu H and Yang H 2019 Thermodynamics and phase transition of a nonlinear electrodynamics black hole in a cavity *J. High Energy Phys.* JHEP07(2019)002
[53] Soleng H H 1995 Charged black points in general relativity coupled to the logarithmic U(1) gauge theory *Phys. Rev.* D **52** 6178–81
[54] Gan Q, Guo G, Wang P and Wu H 2019 Strong cosmic censorship for a scalar field in a Born–Infeld–de Sitter black hole *Phys. Rev.* D **100** 124009
[55] Sheykhi A, Naeimipour F and Zebarjad S M 2015 Thermodynamic geometry and thermal stability of n-dimensional dilaton black holes in the presence of logarithmic nonlinear electrodynamics *Phys. Rev.* D **92** 124054
[56] Ginsparg P H and Perry M J 1983 Semiclassical perdurance of de Sitter space *Nucl. Phys.* B **222** 245–68
[57] Bousso R and Hawking S W 1996 Pair creation of black holes during inflation *Phys. Rev.* D **54** 6312–22
[58] Jansen A 2017 Overdamped modes in Schwarzschild–de Sitter and a Mathematica package for the numerical computation of quasinormal modes *Eur. Phys. J. Plus* **132** 546
[59] Jansen A P Qnmspectral (https://github.com/APJansen/QNMspectral)
[60] Grit (https://centra.tecnico.ulisboa.pt/network/grit/files/ringdown/)
[61] Claudel C-M, Virbhadra K S and Ellis G F R 2001 The Geometry of photon surfaces *J. Math. Phys.* **42** 818–38
[62] Konoplya R A and Zhidenko A 2014 Charged scalar field instability between the event and cosmological horizons *Phys. Rev.* D **90** 064048
[63] Zhu Z, Zhang S-J, Pellicer C E, Wang B and Abdalla E 2014 Stability of Reissner–Nordström black hole in de Sitter background under charged scalar perturbation *Phys. Rev.* D **90** 044042
Zhu Z, Zhang S-J, Pellicer C E, Wang B and Abdalla E 2014 Stability of Reissner–Nordström black hole in de Sitter background under charged scalar perturbation *Phys. Rev.* D **90** 049904